

Surface transformation and inversion domain boundaries in gallium nitride nanorods

Pan Xiao,^{1,a)} Xu Wang,² Jun Wang,² Fujiu Ke,^{1,2} Min Zhou,^{3,4} and Yilong Bai¹

¹*Institute of Mechanics, Chinese Academy of Sciences, Beijing 100190, People's Republic of China*

²*School of Physics, Beihang University, Beijing 100191, People's Republic of China*

³*George W. Woodruff School of Mechanical Engineering, Georgia Institute of Technology, Atlanta, Georgia 30332-0405, USA*

⁴*School of Mechanical and Aerospace Engineering, Seoul National University, Seoul 151-742, Republic of Korea*

(Received 4 October 2009; accepted 3 November 2009; published online 25 November 2009)

Phase transformation and subdomain structure in [0001]-oriented gallium nitride (GaN) nanorods of different sizes are studied using molecular dynamics simulations. The analysis concerns the structure of GaN nanorods at 300 K without external loading. Calculations show that a transformation from wurtzite to a tetragonal structure occurs along $\{01\bar{1}0\}$ lateral surfaces, leading to the formation of a six-sided columnar inversion domain boundary (IDB) in the [0001] direction of the nanorods. This structural configuration is similar to the IDB structure observed experimentally in GaN epitaxial layers. The transformation is significantly dependent on the size of the nanorods. © 2009 American Institute of Physics. [doi:10.1063/1.3268467]

With a wide band gap, gallium nitride (GaN) promises superior performances for blue light-emitting diodes,¹ high-power sources, and optical data storage devices.² Recent advances in the synthesis of one-dimensional nanostructures have brought forth possibilities for GaN to be used in more applications.³ Structural transformations and defects are subjects of active experimental and theoretical research for GaN,⁴ because they lead to significant changes in physical and chemical properties and, therefore, affect applications. These transformations and defects can be caused by external or internal factors. For epitaxially grown GaN layers, because of the lack of a lattice and thermally matching substrate, they always contain large numbers of defects.⁵ High-resolution x-ray diffraction studies of GaN layers have indicated that both carrier mobility and the intensity of photoluminescence are strongly related to defects.⁶ It was also observed that a phase transformation from wurtzite (WZ) to rock-salt structure can be induced by high pressure in GaN.⁷

However for GaN nanostructures, surface stresses due to high surface-to-volume ratios are another factor that may lead to structural transitions. Experimental observations and atomistic simulations show that structural reorientation can occur in metal (copper, silver, and gold) nanowires due to high surface-stresses.^{8,9} This reorientation causes some of the face-centered-cubic metal nanowires to exhibit a shape memory and pseudoelasticity which are not possessed by corresponding bulk materials.⁹ The microscopic details of structural transformations in nanostructures are, however, difficult to investigate through direct experimental observations. Atomistic simulations can play an important role in this regard. Recently, molecular dynamics (MD) simulations are carried out to analyze the atomistic structures of single-crystal GaN nanotubes and the buckling behavior of GaN nanowires.¹⁰ Yet, the effect of surface-stresses on the struc-

tural transformation in GaN nanorods is still poorly understood and merit careful inspection. Here, MD simulations are carried out to investigate the surface transformation and defect formation in GaN nanorods. The analyses concern the equilibrium structure of GaN nanorods with lateral dimensions between 22.6–67.4 Å without external loading. Transformed surface and internal planar defects appear spontaneously during relaxation of the nanorods. To ascertain the relative energetic favorability of the configurations before and after relaxation, free energies of the configurations are independently determined using the molecular statistical thermodynamics (MST) method.¹¹

The computational model simulates configurations observed in experiments.¹² Transmission electron microscopy observations show that as-synthesized GaN nanorods have hexagonal cross sections along the *c*-axis.¹² As illustrated in Fig. 1, the hexagonal, prismatic-shaped nanorod is generated by cutting from the bulk GaN WZ structure with lattice constants $a=3.23$ Å and $c=5.16$ Å. The nanorod has an initial WZ structure with a [0001] axial orientation and $\{01\bar{1}0\}$ lateral surfaces, and we are assuming that the lateral and end surfaces are unreconstructed. To study the size effect, rods with different cross-sectional diameters ($d=22.6, 29.1, 35.5, 42.0, 48.5$, and 61.4 Å) and longitudinal lengths (l , ranging from 36.1 to 516.0 Å) are considered. Since GaN is a cova-

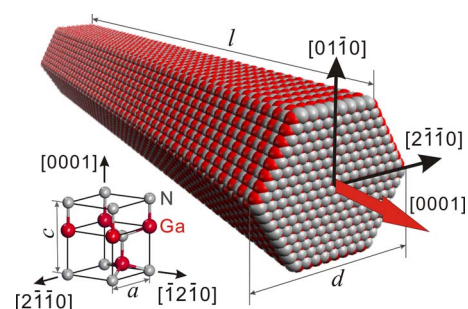


FIG. 1. (Color online) GaN nanorod with the WZ structure.

^{a)} Author to whom correspondence should be addressed. Tel.: 86-010-82543930. FAX: 86-010-82543977. Electronic mail: xiaopan@lnm.imech.ac.cn.

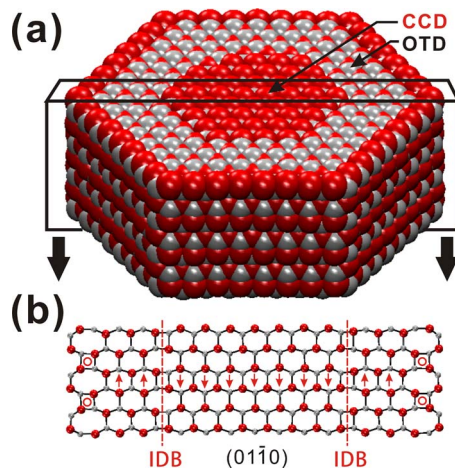


FIG. 2. (Color online) (a) Section of GaN nanorod with two wurtzite-structured domains [the core columnar domain (CCD) and the outer tubular domain (OTD)] separated by an inversion domain boundary (IDB); (b) atomistic arrangement on (01 $\bar{1}$ 0) cross-section showing the structure of the IDB.

lent semiconductor with significant ionic characteristics,¹³ a set of interatomic pair potentials¹⁴ consisting of a long-range Coulombic part and a short-range part is used to describe the Ga–Ga, N–N and Ga–N interatomic interactions. The calculation of long-range Coulomb force uses direct summation without any cutoff in order to accurately describe charge-charge interactions. This scheme is implemented in the LAMMPS code.¹⁵ Traction-free boundary conditions are imposed on the end and lateral surfaces of the nanorods. Structural relaxation occurs under isothermal conditions without external constraints or loading. The temperature of the system is kept at 300 K via velocity scaling. Each calculation lasts 20 ps with a time step of 2 fs to ensure that an equilibrium state is reached.

During the early stages of relaxation, structural transformation nucleates on the {0001} end surfaces and propagates toward the interior of the rod. The transformation reverberations are completed after approximately 2 ps. Subsequently, the rod gradually approaches a thermodynamically equilibrium state without further structural changes. Figure 2(a) shows a section of an equilibrium configuration of the nanorod with $d=48.5$ Å and $l=144.5$ Å. To visualize the details of the transformed structure, the atomic arrangement on the (01 $\bar{1}$ 0) plane is shown in Fig. 2(b). The structures close to the left and right hand sides of the (01 $\bar{1}$ 0) cross-section in Fig. 2(b) (close to the {01 $\bar{1}$ 0} lateral surfaces) of the rod transformed from the original WZ structure to a tetragonal structure (TS). This TS structure contains four-atom rings indicated by the red circles in Fig. 2(b). On the other hand, away from the lateral surfaces, a six-sided columnar boundary is observed in the interior of the rod. This boundary is along the {01 $\bar{1}$ 0} facets of the WZ structure and contains the [0001] direction. Because of this previously nonexistent domain boundary, the interior (other than the transformed lateral surfaces with the TS structure) of the nanorod in Fig. 2(a) is divided into two WZ domains [a core columnar domain (CCD) and an outer tubular domain (OTD)], as seen in Figs. 2(a) and 2(b). Note that the polarity of the CCD is opposite to that of the OTD [Fig. 2(b)]. Because of this orientation inversion, the defect in the form of the surface

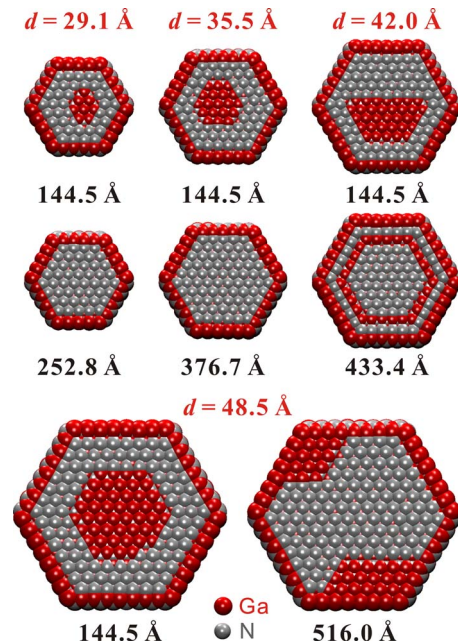


FIG. 3. (Color online) Inversion domain boundary distributions in GaN nanorods of different lateral dimensions (d) and lengths (below each pattern).

boundary between the two domains is called an inversion domain boundary or IDB.¹⁶ The IDBs in the nanorods analyzed here also have the TS structure which is similar to the TS obtained in zinc oxide nanorods under tensile loading.¹⁷ It should be mentioned that structural transformations also occur near the {0001} end surfaces, so IDBs may not be directly observed at the end surfaces.

Similar IDBs have been observed in GaN epilayers,^{16,18} and the IDBs in the GaN epilayers are also along the c -axis and occupy hexagonal regions bounded by {01 $\bar{1}$ 0} planes. Two models have been proposed for the atomistic configurations for these IDBs. The first is the H model¹⁸ and the second is the V model.¹⁶ The structure observed here is similar to the later. First-principles calculations by Northrup *et al.*¹⁹ show that the domain wall energy for the V-type IDB (denoted as IDB* in Ref. 19) is approximately 0.025 eV/Å² (0.019 eV/Å² according to the empirical potential used in our simulations), which is much lower than the energy of 0.167 eV/Å² for the H-type IDB.

The effects of rod size (both lateral diameter and length) on the transformation and IDB structure are also analyzed. We first focus on the effect of lateral dimension d . Six GaN nanorods with the same length (144.5 Å) but different lateral diameters (22.6, 29.1, 35.5, 42.0, 48.5, and 61.4 Å) are simulated. All six cases show transformed lateral surfaces. However, the IDB structure appears only in larger rod sizes and not in the rod with $d=22.6$ Å. For the transformed rods with IDBs (see in Fig. 3; rods with $d=22.6$ and 61.4 Å are not shown), the IDBs have different shapes but still remain {01 $\bar{1}$ 0} facets of the WZ structure. The fraction of the rod's cross-sectional area that is occupied by the CCD (γ) is defined as a measure for the size of the IDBs. This measure increases from 12.0% to 29.8% as the lateral dimension d increases from 29.1 to 61.4 Å. A GaN nanofilm with thickness along the c -axis equal to 144.5 Å (same as the length of nanorods) is taken as the limiting case for nanorods as the

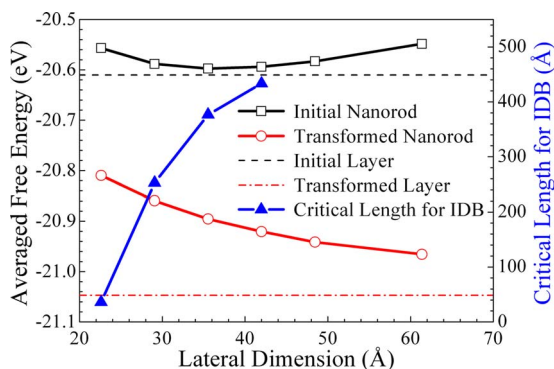


FIG. 4. (Color online) Average free energies per atom for the initial and transformed configurations of GaN layers and nanorods of the same length (144.5 Å) at different lateral dimensions, also shown is the critical length below which the IDB is observed in GaN nanorods.

lateral size approaches infinity. Numerically, this is achieved by imposing periodic boundary conditions along the lateral surfaces. Consistent with experiments on nanofilms, IDBs are observed in the calculation for the nanofilm as well. The length of the rods is, especially, an important factor affecting the transformations. Specifically, as the length of the rod with $d=29.1$ Å increases from 144.5 to 252.8 Å, the WZ-TS transformation still occurs at the lateral surfaces but no IDB is formed (see Fig. 3). The critical length for observing the IDB in rods with d ranging from 22.6 to 42.0 Å is plotted in Fig. 4. This critical length increases dramatically as the lateral dimension d increases. The critical length for the rod with $d=22.6$ Å is about 36.1 Å, giving an explanation why IDB is not observed in the rod with $l=144.5$ Å as mentioned above. Structural transformations in GaN nanorods become more complex as size increases. Although no IDB forms in the rod with $d=42.0$ Å and $l=433.4$ Å as shown in Fig. 3, a ring of atoms with a structure similar to the structure of the lateral surfaces is seen. For the rods with $d=48.5$ Å, length has a significant impact as well, with the IDBs in the longer rod ($l=516.0$ Å) connected to the transformed surfaces without an OTD like that in the shorter rod ($l=144.5$ Å). Since no external loading is applied, this size-dependence of behavior can be partly attributed to differences in surface stresses in the nanorods. As size increases, the effect of surface stresses decreases since the surface-to-volume ratio becomes lower. The IDBs disappear completely when the dimensions (diameter and length) are large enough and the surface stress is no longer high enough to drive the structural transformations. To demonstrate this point, rods with an effective limit of infinite length (approximated through periodic boundary conditions along the c -axis) is analyzed. As expected, no structural transformation is observed and the whole rod remains in the WZ structure regardless of lateral size.

To confirm that the IDB structure of the nanorods is indeed energetically favored, the Helmholtz free energies of the configurations before and after relaxations are analyzed. To this end, the MST method based on statistical thermodynamics and lattice dynamics is used.¹¹ This method treats

atoms in an isothermal-isochoric solid system as harmonic oscillators and allows the Helmholtz free energy to be evaluated. The per-atom free energies of the initial and transformed configurations are plotted in Fig. 4. Clearly in all cases, the transformed structure with the IDB has a lower free energy than the initial structure. Therefore, the transformed structure with the reorganized surfaces and the IDB is indeed energetically favored.

In summary, MD and MST calculations show that GaN nanorods with length equal to 144.5 Å and lateral dimensions greater than 22.61 Å and nanofilms with single-crystalline WZ structures are not stable and the energetically favored configurations for $d \geq 29.07$ Å involve reorganized surfaces and internal IDBs. The MD simulations also reveal a dependence of the phenomenon on size. This size-dependence of the formation of IDBs is attributed to differences in surface stresses of nanorods with different surface-to-volume ratios.

Support from the NSFC (Grant Nos. 10772012 and 10732090), NBRPC (Grant No. 2007CB814800), and KOSEF (Grant No. R31-2008-000-10083-0) is acknowledged. Computations are carried out at the CNIC Supercomputing Center, the LSEC of the CAS, and on the DPRL cluster at Georgia Tech.

¹S. Nakamura, T. Mukai, and M. Senoh, *Appl. Phys. Lett.* **64**, 1687 (1994).

²H. Y. Cha, H. Q. Wu, S. Chae, and M. G. Spencer, *J. Appl. Phys.* **100**, 024307 (2006).

³H. Morkoc and S. N. Mohammad, *Science* **267**, 51 (1995); F. A. Ponce and D. P. Bour, *Nature (London)* **386**, 351 (1997); Y. S. Park, C. M. Park, D. J. Fu, T. W. Kang, and J. E. Oh, *Appl. Phys. Lett.* **85**, 5718 (2004).

⁴B. Garni, J. Ma, N. Perkins, J. T. Liu, T. F. Kuech, and M. G. Lagally, *Appl. Phys. Lett.* **68**, 1380 (1996); A. R. Smith, R. M. Feenstra, D. W. Greve, M. S. Shin, M. Skowronski, J. Neugebauer, and J. E. Northrup, *ibid.* **72**, 2114 (1998).

⁵V. Potin, P. Vermaut, P. Ruterana, and G. Nouet, *J. Electron. Mater.* **27**, 266 (1998).

⁶J. Y. Shi, L. P. Yu, Y. Z. Wang, G. Y. Zhang, and H. Zhang, *Appl. Phys. Lett.* **80**, 2293 (2002).

⁷P. Perlin, C. Jaubertiecarillon, J. P. Itie, A. S. Miguel, I. Grzegory, and A. Polian, *Phys. Rev. B* **45**, 83 (1992); S. Limpijumnong and W. R. L. Lambrecht, *Phys. Rev. Lett.* **86**, 91 (2001).

⁸J. Diao, K. Gall, and M. L. Dunn, *Nature Mater.* **2**, 656 (2003).

⁹H. S. Park, K. Gall, and J. A. Zimmerman, *Phys. Rev. Lett.* **95**, 255504 (2005); W. Liang and M. Zhou, *Phys. Rev. B* **73**, 115409 (2006).

¹⁰B. Xu, A. J. Lu, B. C. Pan, and Q. X. Yu, *Phys. Rev. B* **71**, 125434 (2005).

¹¹H. Y. Wang, M. Hu, M. F. Xia, F. J. Ke, and Y. L. Bai, *Int. J. Solids Struct.* **45**, 3918 (2008).

¹²L. W. Tu, C. L. Hsiao, T. W. Chi, I. Lo, and K. Y. Hsieh, *Appl. Phys. Lett.* **82**, 1601 (2003).

¹³R. Pandey, J. E. Jaffe, and N. M. Harrison, *J. Phys. Chem. Solids* **55**, 1357 (1994).

¹⁴P. Zapol, R. Pandey, and J. D. Gale, *J. Phys.: Condens. Matter* **9**, 9517 (1997).

¹⁵P. Steve, *J. Comput. Phys.* **117**, 1 (1995).

¹⁶L. T. Romano, J. E. Northrup, and M. A. Okeefe, *Appl. Phys. Lett.* **69**, 2394 (1996).

¹⁷J. Wang, A. J. Kulkarni, K. Sarasamak, S. Limpijumnong, F. J. Ke, and M. Zhou, *Phys. Rev. B* **76**, 172103 (2007).

¹⁸V. Potin, G. Nouet, and P. Ruterana, *Appl. Phys. Lett.* **74**, 947 (1999).

¹⁹J. E. Northrup, J. Neugebauer, and L. T. Romano, *Phys. Rev. Lett.* **77**, 103 (1996).